



Research article

Imidazolium based ionic liquid derivatives; synthesis and evaluation of inhibitory effect on mild steel corrosion in hydrochloric acid solution



N. Subasree, J. Arockia Selvi*

Department of Chemistry, SRM Institute of Science and Technology, Kattankulathur, Tamil Nadu, 603203, India

ARTICLE INFO

Keywords:

Materials chemistry
Physical chemistry
Ionic liquids
Inhibitor
Mild steel
Adsorption
AFM

ABSTRACT

Imidazolium bearing ionic liquids (ILs), 3-hexadecyl-1-methyl-1H-imidazol-3-ium bromide [C₁₆M₁Im] [Br] and 3-hexadecyl-1,2-dimethyl-1H-imidazol-3-ium bromide [C₁₆M₂Im] [Br] have been synthesized. These compounds were evaluated for corrosion resistance of mild steel in 1M HCl solution by gravimetric and electrochemical studies. The results were noticed that the inhibition efficiency, has enhanced due to a rise in the concentration of inhibitor. Further, it is observed that [C₁₆M₂Im] [Br] inhibition efficiency better than [C₁₆M₁Im] [Br] due to the increased alkyl substituents. Polarization study reveals that the used inhibitors behave as a mixed type, but predominantly exhibited the anodic inhibitive effect. The inhibitors adsorbed on the metal surface obeys Langmuir adsorption isotherm. Surface topography examined using an Atomic Force Microscope (AFM) and a Scanning Electron Microscope (SEM) with EDAX analyses. The formation of the Fe-inhibitor complex on mild steel surface has been confirmed by UV-Visible spectroscopy.

1. Introduction

Mineral acids are, particularly hydrochloric acid, commonly used in numerous industrial applications, such as, acid pickling, acid descaling, and other petrochemical processes [1, 2], which causes serious corrosive damage of the steel materials. The use of corrosion inhibitors is the most effective method to protect the metal from corrosion [3, 4, 5]. Organic compounds commonly serve as inhibitors and inhibit metal from corrosion by a protective layer formed on the metal surface due to their active centers, especially heteroatoms (N, S and O) and double/triple bonds which concerning their interaction with the metal surface [6, 7, 8, 9, 10]. Moreover, ionic liquids are molten salts contain organic cation and different anion, which could be melt at/or below room temperature [11, 12]. The ionic liquids are also employed as green and sustainable replacements for volatile organic compounds due to their physicochemical properties [13]. Recently, ionic liquids have been utilized as inhibitors to prevent metal corrosion in acidic media [14, 15, 16, 17]. It was interpreted that the adsorption of such inhibitors on the metal surface relies upon the specific interactions [18, 19] due to free electrons, C=N- group, the electron density of the nitrogen atom and high alkyl chain length present in the molecule [20, 21, 22].

Imidazole based ionic liquids is one of the most important classes of ionic liquids as they have numerous advantages such as safety, low cost,

non-toxic, biodegradable, soluble in water, strong adsorption on metal and high protection efficiency [23]. Generally, inhibition performance of imidazole based ionic liquids depends on their alkyl chain length and their size [24]. By increasing the number of the alkyl chain, the corrosion rate decreases in the presence of the inhibitor indicate inhibitor adsorption on the metal surface and thus inhibits metal from corrosion [25]. Also, the presence of free nitrogen atom in an imidazole compound develops a film on the metal surface which is usually hydrophobic, thus the hydrophobic film reduces the attack by the chloride ions or any corrosive environment on the metal surface. These can be added as effective corrosion inhibitors in fire water which contain mostly chloride ions is the proposed recommendation for corrosion protection of entire fire water piping services [26].

From the above observations, we report the inhibition of mild steel in 1M HCl medium using two imidazolium ionic liquids namely, 3-hexadecyl-1-methyl-1H-imidazol-3-ium bromide [C₁₆M₁Im] [Br] and 3-hexadecyl-1,2-dimethyl-1H-imidazol-3-ium bromide [C₁₆M₂Im] [Br]. This study is to examine the effect of increased numbers of the methyl group substituent in imidazolium ionic liquids with high alkyl chain length on the protection capacity against corrosion of mild steel. The performance of the inhibition was studied by the weight loss method at different temperature. The Langmuir adsorption isotherm was used to give evidence to inhibitors adsorbed on mild steel. UV spectra used to study the

* Corresponding author.

E-mail address: arockiaj@srmist.edu.in (J.A. Selvi).

interaction between inhibitors and mild steel. SEM-EDAX and AFM study were used to study the changes that occur on the metal surface with and without inhibitors. The chemical structures of [C₁₆M₁Im] [Br] and [C₁₆M₂Im] [Br] were shown in Figures 1 and 2.

2. Experimental section

2.1. Materials and methods

A corrosive test solution of 1M HCl was prepared using an analytical grade of HCl at 36% with distilled water. The elemental composition of mild steel was analyzed by an optical emission spectrometer (in % by weight) chosen in the present study given in Table 1. The size of mild steel used for weight loss and electrochemical studies is rectangular in shape with dimension of 10 × 4 × 2 cm², while for the surface study's cubic size with a dimension of 1 × 1 cm² were used. The mild steel samples were abraded with the sandpaper grade (400–1200), cleaned with acetone, rinsed with double distilled water, finally dried and weighed.

2.2. Synthesis of inhibitors

The synthesis of [C₁₆M₁Im] [Br] and [C₁₆M₂Im] [Br] was prepared according to the previous literature [27]. The products were characterized by ¹H NMR and FT-IR spectroscopy [Figures 3, 4, and 5].

2.2.1. Preparation of [C₁₆M₁Im] [Br] and [C₁₆M₂Im] [Br]

1-methyl imidazole or 1,2-dimethyl imidazole (10 mmol) was mixed with 35mL of CH₃CN by stirring continuously. (12 mmol) of 1 bromohexadecane was added into the above stirred solution drop wise. The mixed solution was heated to 80 °C and was refluxed for 48 h with continuous stirring in N₂ atmosphere. The crude product was washed a few times with dry acetonitrile and dried overnight under a vacuum at 70 °C. The corresponding synthetic route was shown in Scheme 1.

[C₁₆M₁Im] [Br]: ¹H NMR (500 MHz, DMSO) δ 9.05 (s, 1H), 7.70 (s, 1H), 7.63 (s, 1H), 4.12 (t, *J* = 7.2 Hz, 2H), 3.83 (s, 3H), 1.79–1.69 (m, 2H), 1.19 (s, 29H); IR (cm⁻¹) 3065(C–H), 1461–1627(C=C), 1167(C–N). [C₁₆M₂Im] [Br]: ¹H NMR (500 MHz, DMSO) δ 7.59 (m, 2H), 4.07 (t, *J* = 7.2 Hz, 2H), 3.74 (s, 3H), 2.55 (s, 3H), 1.66 (m, 2H), 1.38–0.99 (m, 29H); IR (cm⁻¹) 3049(C–H), 1461–1580 (C=C), 1111(C–N).

2.3. Weight loss studies

Weight loss experiments have been carried out on mild steel specimens, which were immersed in 100ml of 1M HCl solution with and without five different concentrations of [C₁₆M₁Im] [Br] and [C₁₆M₂Im] [Br] for 1 h at different temperatures (298K, 308K, 318K and 328K). After 1 h, the immersed mild steel samples were removed, washed and reweighed. From the weight difference values used to calculate for corrosion rate (CR) and inhibition efficiency (IE %) from the following equations,

$$IE (\%) = \frac{W_B - W_I}{W_B} \times 100 \quad (1)$$

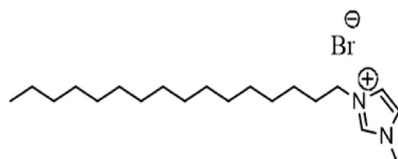


Figure 1. Chemical structure of [C₁₆M₁Im] [Br].

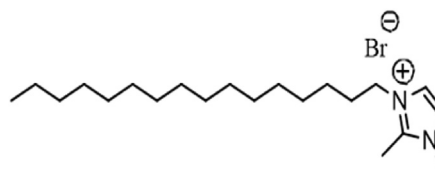


Figure 2. Chemical structure of [C₁₆M₂Im] [Br].

$$CR(mmpy) = \frac{87.6 \times W}{ATD} \quad (2)$$

Where, W_B and W_I are the weight loss values for mild steel in 1M HCl in the absence and presence of inhibitors. W is the weight loss in mg, A is the immersed area of the mild steel sample (cm²), T is the immersion period in an hour and D is the density of the used metal sample.

2.4. Electrochemical studies

Electrochemical studies were performed using Bio-Logic SP 300 through a conventional three electrode system which has a mild steel sample as a working electrode, platinum wire and Hg/HgCl₂ become counter and reference electrodes respectively. These electrodes were immersed in 1M HCl at different concentrations of [C₁₆M₁Im] [Br] and [C₁₆M₂Im] [Br], separately. Polarization experiments were performed from a potential range of ±250 mV at a scanning rate of 1 mV/S. Impedance experiments were performed in the frequency range from 100000 HZ to 0.010 HZ by using amplitude of 10mV. The results have been fitted with EC Laboratory software.

2.5. UV analysis

The UV-Visible spectra of the inhibitor solution were recorded before and after immersion in mild steel. The formation of the metal-inhibitor complex was studied using UV-Visible spectrometry (UV-Visible spectrophotometer of the double beam laboratory instrument by Labmann Pvt. Ltd).

2.6. Surface analysis

Surface studies were carried out using high-resolution field emission scanning electron microscope (FESEM) FEI quanta FEG 200 with an energy dispersive X-ray analyzer. Scanning electron microscopy (SEM) used to study the surface morphology of the mild steel specimen in the absence and presence of 250ppm of inhibitors for 1hour at room temperature. Energy dispersive X-ray analyzer (EDAX) was used to study the chemical composition of the test specimens. Atomic force microscopy (AFM) studies were performed using the Scanning Probe Microscope 5100 Pico LE (Agilent Technologies).

3. Results and discussions

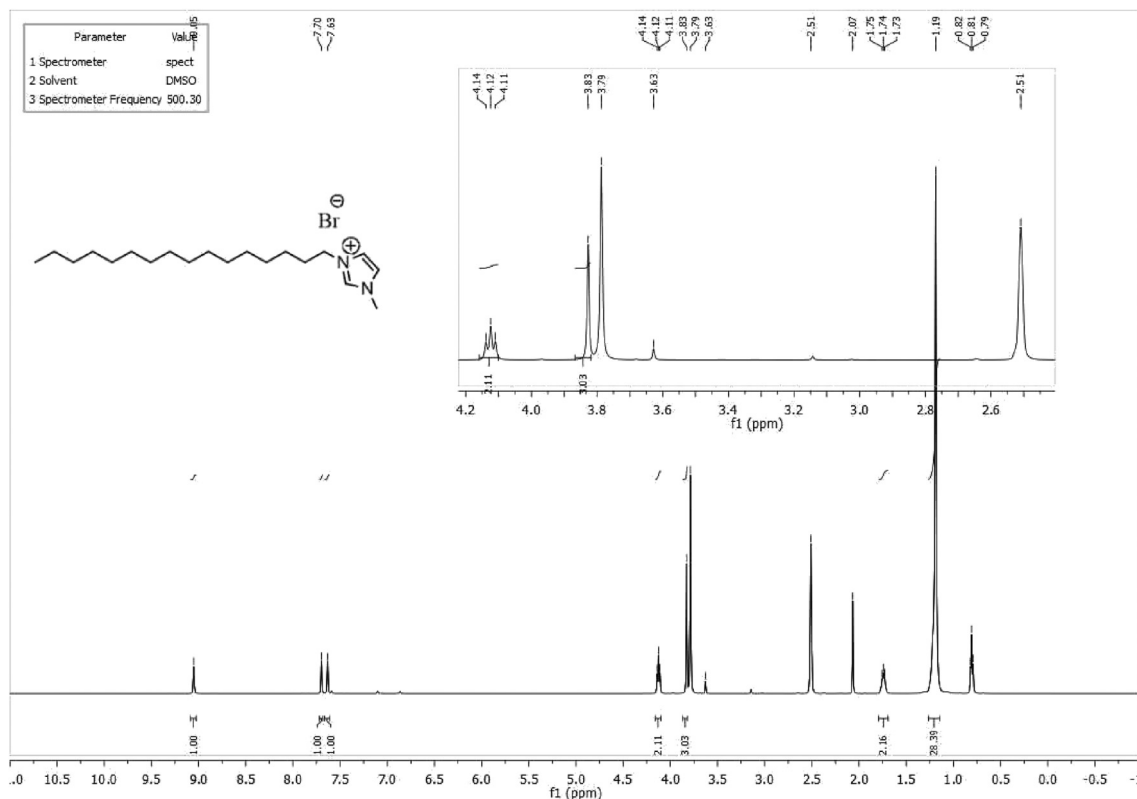
3.1. Weight loss experiment

3.1.1. Effect of inhibitor concentration

From the weight loss experiments, the calculated values of the corrosion rate (CR) and the inhibition efficiency (IE %) were attained with the addition of different concentrations of [C₁₆M₁Im] [Br] and [C₁₆M₂Im] [Br] after 1h immersion of mild steel in 1M HCl at 298K are listed in the Table 2. Before and after 1h immersion of the mild steel specimen are shown in Figure 6. The values of inhibition efficiency, increased with increasing inhibitor concentration, which due to increasing the concentration of inhibitor raised the availability of heteroatom such as N, methyl substituent and imidazole ring, which supports the highest concentration of used inhibitors effectively covered on the metal surface. On the other hand, increasing concentration of

Table 1. The chemical composition of the studied mild steel specimen (in weight %).

C	Mn	P	Si	Cr	S	Fe
0.067	1.65	0.02	0.145	0.198	0.006	Balance

**Figure 3.** ^1H NMR of $[\text{C}_{16}\text{M}_1\text{Im}] [\text{Br}]$.

inhibitor decreased the corrosion rate because in the presence of inhibitor could affect either or both metal dissolution and hydrogen evolution processes [28]. The highest inhibition efficiency of 90.67% and 95.35% respectively at 500ppm of $[\text{C}_{16}\text{M}_1\text{Im}] [\text{Br}]$ and $[\text{C}_{16}\text{M}_2\text{Im}] [\text{Br}]$. Inhibitor $[\text{C}_{16}\text{M}_2\text{Im}] [\text{Br}]$ achieved the higher inhibition efficiency due to the presence of additional methyl group substituents with respect to the $[\text{C}_{16}\text{M}_1\text{Im}] [\text{Br}]$. It is remarkable that $[\text{C}_{16}\text{M}_2\text{Im}] [\text{Br}]$ is strongly adsorbed on the metal surface than $[\text{C}_{16}\text{M}_1\text{Im}] [\text{Br}]$. $[\text{C}_{16}\text{M}_2\text{Im}] [\text{Br}]$ of increased methyl substituent can effectively protect corrosion due to increase in electron density of inhibitor molecule. Therefore, this compound is more stable and inhibits the metal surfaces [29, 30]. Compared to the previous literature, the imidazolium based corrosion inhibitors listed in the Table 3, $[\text{C}_{16}\text{M}_1\text{Im}] [\text{Br}]$ and $[\text{C}_{16}\text{M}_2\text{Im}] [\text{Br}]$ shows better inhibition efficiency. These phenomena are related to the effect of methyl substituent, high alkyl chain length and the heteroatom present in the inhibitors.

3.1.2. Temperature effect

The values of inhibition efficiency from weight loss experiments at different temperature (298K, 308K, 318K & 328K) are presented in Table 2. From the Table 2, the efficiency of the inhibitory molecules depends on their concentration and temperature [31]. The inhibition efficiency of $[\text{C}_{16}\text{M}_1\text{Im}] [\text{Br}]$ and $[\text{C}_{16}\text{M}_2\text{Im}] [\text{Br}]$ on mild steel was found to be reduced with rising temperatures. This can be described by the disruption of inhibitors of metal surface. The inhibition efficiency decreases up to 328K temperature suggests physical adsorption occurrence between the studied inhibitors and mild steel [32]. Hence the inhibitors

attained maximum inhibition efficiency at 298K. In addition the corrosion rate values favoured the corrosion inhibiting nature of the inhibitors.

3.1.3. Adsorption isotherm

The adsorption isotherm study interprets the interaction between the inhibitory molecules and the metal surface. Surface coverage values (θ) of weight loss experiments were used to study the adsorption isotherm (Temkin, Freundlich and Langmuir) and it was found that they obey Langmuir adsorption isotherm. The graph of the C/θ VS concentration of the inhibitor yielded a straight line shown in Figure 7. The K_{ads} values of used inhibitors were calculated by the following equation,

$$\frac{C}{\theta} = \frac{1}{K_{ads}} + C \quad (3)$$

Where C is the concentration of the inhibitor, θ is the surface coverage and K_{ads} represents the equilibrium constant of adsorption. K_{ads} value is calculated from the intercept of the Figure 7. The high value of K_{ads} obtained for use inhibitors reflects efficient adsorption. The K_{ads} value is higher for $[\text{C}_{16}\text{M}_2\text{Im}] [\text{Br}]$ indicates their adsorption capability of mild steel surface was stronger than $[\text{C}_{16}\text{M}_1\text{Im}] [\text{Br}]$. From the Table 4, clearly shown K_{ads} decrease with increasing temperature, which indicates adsorbed inhibitors on a metal surface that can be desorbed with rising temperatures.

The free energy of adsorption (ΔG^0_{ads}) can be calculated by following equation,

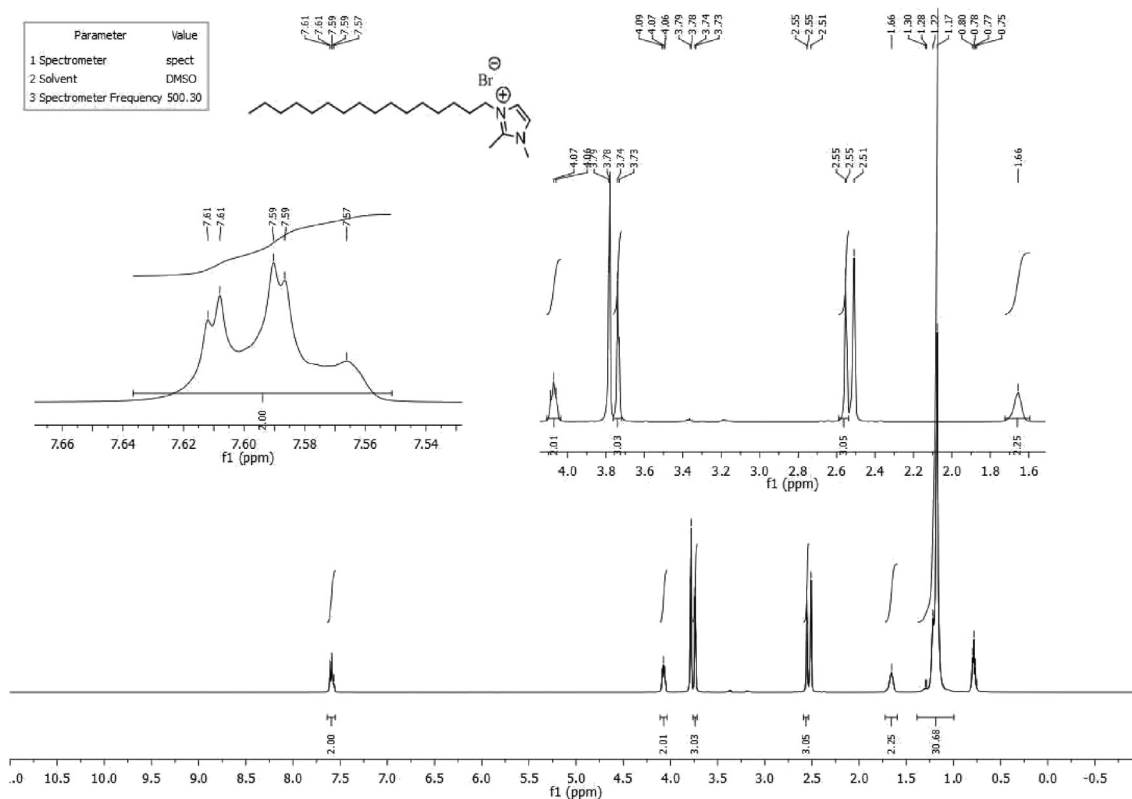


Figure 4. ¹H NMR of [C₁₆M₂Im] [Br].

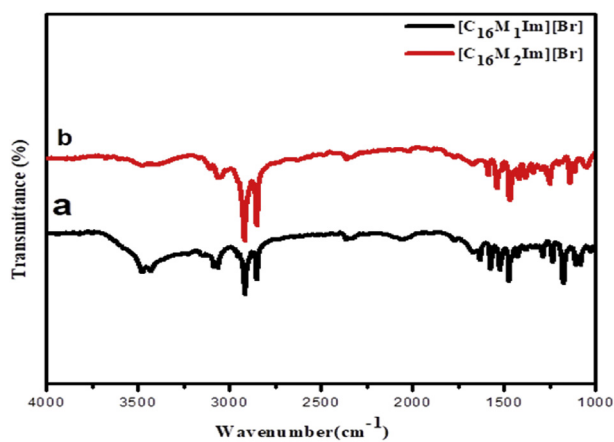
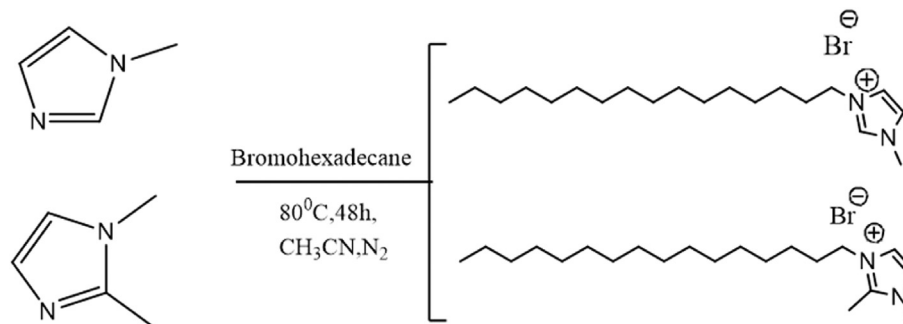


Figure 5. FT-IR spectra of [C₁₆M₁Im] [Br] and [C₁₆M₂Im] [Br].



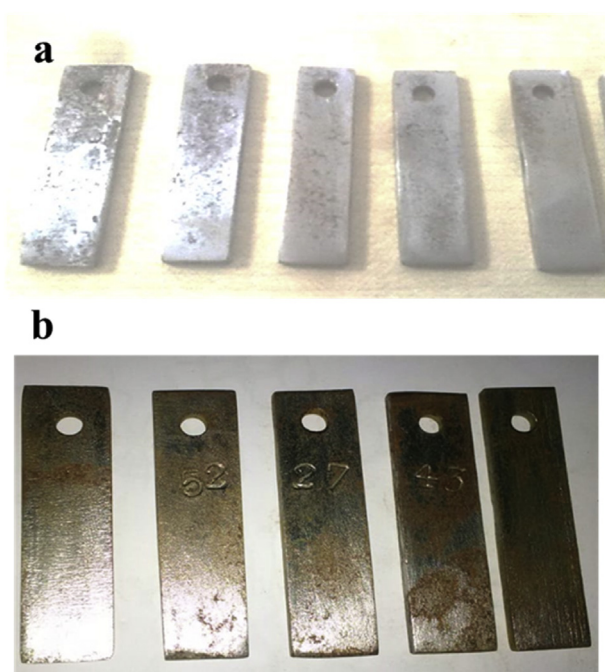
Scheme 1. Synthesis scheme of [C₁₆M₁Im] [Br] and [C₁₆M₂Im] [Br].

$$\Delta G^{\circ}_{\text{ads}} = -RT \ln(55.5 K_{\text{ads}}) \quad (5)$$

Where R is the universal gas constant, T is the absolute temperature in K and the 55.5 value represents the concentration of water solution in mol L⁻¹. Generally, $\Delta G^{\circ}_{\text{ads}}$ values of -20 K J mol⁻¹ or less are responsible for electrostatic interaction between the inhibitor and mild steel surface (physisorption) and the values of -40 K J mol⁻¹ or more negative are responsible for charge transfer between inhibitor and mild steel surface (chemisorption) were demonstrated by yesudass et al [36]. In this present work, the obtained value of $\Delta G^{\circ}_{\text{ads}}$ is lower than -20 K J mol⁻¹, which indicates physical adsorption. Therefore, it is concluded that the studied inhibitors were physically adsorbed on the metal surface. Meanwhile, the negative values of $\Delta G^{\circ}_{\text{ads}}$ for the inhibitors provide spontaneous adsorption process occurring on the mild steel surface. The inhibition efficiency decreases with increase in temperature, which is attributed due to physisorption of inhibitor molecules mainly depends on the electron density of the donor atom and the structure e molecule [37]. The physisorption is further confirmed from adsorption isotherm.

Table 2. Weight loss results of mild steel in 1M HCl with and without different concentrations of [C₁₆M₁Im] [Br] and [C₁₆M₂Im] [Br] at different temperatures.

Inhibitor (ppm)	298K		308K		318K		328K	
	CR (mmpy)	IE (%)						
BLANK	4.79	-	5.90	-	6.90	-	7.91	-
[C ₁₆ M ₁ Im] [Br]								
50	2.11 ± 0.05	55.81	2.78 ± 0.02	52.83	3.67 ± 0.06	46.77	4.34 ± 0.03	45.07
100	1.78 ± 0.03	62.79	2.45 ± 0.04	58.50	3.23 ± 0.06	53.24	3.67 ± 0.02	53.52
150	1.33 ± 0.03	72.09	2.00 ± 0.02	66.04	2.67 ± 0.07	61.29	3.23 ± 0.02	59.15
200	0.89 ± 0.01	81.40	1.67 ± 0.01	71.70	2.22 ± 0.04	67.74	3.00 ± 0.06	61.97
250	0.44 ± 0.02	90.67	1.11 ± 0.02	81.13	1.89 ± 0.01	72.58	2.67 ± 0.04	66.20
[C ₁₆ M ₂ Im] [Br]								
50	2.00 ± 0.08	58.14	2.67 ± 0.02	54.72	3.34 ± 0.08	51.61	4.23 ± 0.05	46.48
100	1.22 ± 0.02	74.41	2.34 ± 0.09	60.38	3.00 ± 0.07	56.45	3.56 ± 0.08	54.93
150	1.00 ± 0.07	79.07	1.78 ± 0.07	69.81	2.56 ± 0.04	62.90	3.12 ± 0.02	60.56
200	0.78 ± 0.07	83.72	1.56 ± 0.02	73.58	2.11 ± 0.01	69.35	2.67 ± 0.07	66.20
250	0.22 ± 0.04	95.35	1.00 ± 0.11	83.02	1.67 ± 0.03	75.81	2.22 ± 0.02	71.83

**Figure 6.** a) Before and b) after immersion Mild steel specimens.

3.2. Potentiodynamic polarization studies

Polarization curves for mild steel in 1M HCl in the presence and absence of different concentrations of [C₁₆M₁Im] [Br] and [C₁₆M₂Im] [Br] are shown in Figure 8. The Polarization parameters including the corrosion potential (E_{corr}), corrosion current density (I_{corr}), cathodic tafel slope (β_c), anodic tafel slope (β_a) and the inhibition efficiency (IE %) were listed in Table 5. The inhibition efficiency (IE %) is calculated using the following equations,

$$IE (\%) = \frac{I_{\text{corr}}' - I_{\text{corr}}}{I_{\text{corr}}'} \times 100 \quad (7)$$

Where, I_{corr}' and I_{corr} are mild steel in 1M HCl in the absence and presence of various concentrations of inhibitors, respectively.

I_{corr} values decrease with the addition of increasing inhibitor concentrations, this suggests the inhibiting nature of C₁₆M₁Im [Br] and [C₁₆M₂Im] [Br]. From the figure and table, there is no significant change in the values of anodic and cathodic Tafel slopes, suggesting that the used inhibitors are mixed type and protect the metal from corrosion by blocking the active sites of the metal surface. According to the literature, a shift in E_{corr} values is more than 85 mV with respect to E_{corr} of the blank, the inhibitor was considered as a cathodic or anodic type and the shift is less than 85mV, the inhibitor can be considered as a mixed type [38]. In the present work studied inhibitors, E_{corr} value shift was observed at positive side, the displacement was not more than 85mV, which reveals that studied inhibitors are mixed type but predominantly exhibited anodic. The highest inhibition efficiency of 87.12 % was obtained by [C₁₆M₂Im] [Br] and the lowest inhibition efficiency of 78.74% were attained by [C₁₆M₁Im] [Br]. Inhibition efficiency was found to be the following order, [C₁₆M₂Im] [Br] > [C₁₆M₁Im] [Br].

3.3. Electrochemical impedance spectroscopy

Impedance spectroscopy and bode plots for mild steel immersed in 1M HCl in the absence and the presence of various concentrations of

Table 3. Comparison study of inhibition efficiency of [C₁₆M₁Im][Br] and [C₁₆M₂Im][Br] with the previous literature data as a corrosion inhibitor for mild steel in HCl solution.

Inhibitor	Medium	IE (%)	Ref
[C ₁₆ M ₁ Im] [Br]	1M HCl	90.6	Present work
[C ₁₆ M ₂ Im] [Br]	1M HCl	95.5	Present work
3-(3-phenylpropyl)-1-propyl-1H-imidazol-3-ium bromide	1M HCl	92.3	[33]
3-(4-phenoxybutyl)-1-propyl-1H-imidazol-3-ium bromide	1M HCl	94.2	[33]
1-butyl-3-methylimidazolium bromide	1M HCl	56.5	[34]
1-hexyl-3-methylimidazolium bromide	1M HCl	85.5	[34]
1-vinyl-3-aminopropylimidazolium hexafluorophosphate	1M HCl	86.9	[35]
1-vinyl-3-aminopropylimidazolium tetrafluoroborate	1M HCl	63.9	[35]

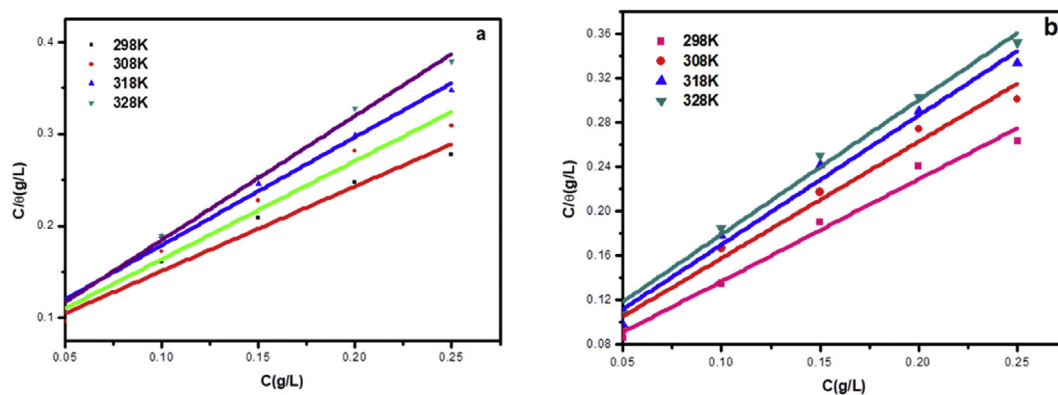


Figure 7. Langmuir adsorption isotherm of a) $[C_{16}M_1Im][Br]$ ($R^2 = 0.9943$) b) $[C_{16}M_2Im][Br]$ ($R^2 = 0.9982$) on mild steel surface in 1M HCl at room temperature.

Table 4. K_{ads} and ΔG^0_{ads} of adsorption of mild steel in 1M HCl with $[C_{16}M_1Im][Br]$ and $[C_{16}M_2Im][Br]$ at different temperatures.

Inhibitor (ppm)	T (K)	K_{ads} ($L g^{-1}$)	ΔG^0_{ads} ($KJmol^{-1}$)
$[C_{16}M_1Im][Br]$	298	16.8890	-16.95
	308	17.5685	-17.62
	318	16.2258	-17.98
	328	20.0964	-19.13
$[C_{16}M_2Im][Br]$	298	22.1533	-17.62
	308	18.9071	-17.81
	318	18.6115	-18.31
	328	17.1556	-18.70

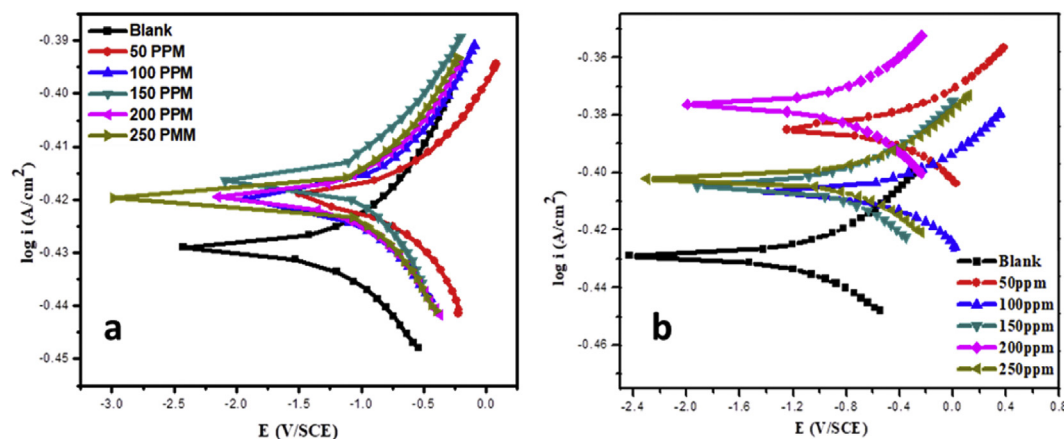


Figure 8. Polarization curves for mild steel in 1M HCl in the absence and presence of different concentrations of a) $[C_{16}M_1Im][Br]$ and b) $[C_{16}M_2Im][Br]$.

$[C_{16}M_1Im][Br]$ and $[C_{16}M_2Im][Br]$ respectively shown in Figures 9 and 10. In the presence of an inhibitor, the size of the semicircle is greater than that of the uninhibited system. From the figure, it is clearly seen that the size of the semicircle increased with increasing concentration of inhibitors. This revealed that the mild steel specimen was protected against corrosion in the inhibited system. This shows an increase in R_{ct} values [39]. From the bode plots shown in Figure 10, we found that only one time constant exists for $[C_{16}M_1Im][Br]$ and $[C_{16}M_2Im][Br]$, due to the fact that only one phase angle peak close to more negative directions as the result of increasing inhibitor concentrations. This was attributed to inhibitor molecules adsorbed on the mild steel surface. Meanwhile, the more negative phase angle value indicates the greater inhibitive behavior due to the high concentration of inhibitor molecules adsorbed. The impedance parameters double layer capacitance (C_{dl}), charge transfer resistance (R_{ct}) and inhibition efficiency (IE %) are listed in Table 6. The

inhibition efficiency and the double layer capacitance values are calculated by the following equations

$$C_{dl} = \frac{1}{2\pi f_{max} R_{ct}} \tag{6}$$

$$IE \% = \frac{R'_{ct} - R_{ct}}{R'_{ct}} \times 100 \tag{7}$$

Where f_{max} is the maximum impedance frequency, R'_{ct} and R_{ct} are the charge transfer values with and without inhibitors respectively.

As shown in the table, the R_{ct} values are high for mild steel in 1M HCl in the inhibited system, illustrating the inhibitor layer formed on the mild steel surface due to the charge transfer process. Furthermore, C_{dl} values decrease with increasing inhibitor concentration, which is attributed to that inhibitors get adsorbed on the mild steel surface [40]. As a result

Table 5. The potentiodynamic polarization parameters for mild steel in 1M HCl in the presence and absence of different concentrations of inhibitors.

Inhibitor (ppm)	E_{corr} (mV)	I_{corr} ($\mu A cm^{-2}$)	β_a (mVdec ⁻¹)	β_c (mVdec ⁻¹)	IE (%)
BLANK	-429	254.73	74	88	-
[C₁₆M₁Im][Br]					
50	-444	192.45	36	35	24.40
100	-432	106.17	32	21	58.26
150	-419	83.10	40	30	67.32
200	-418	67.69	34	26	73.62
250	-452	54.59	31	33	78.74
[C₁₆M₂Im][Br]					
50	-450	186.10	41	36	26.77
100	-409	122.21	34	31	51.96
150	-406	107.08	38	42	57.87
200	-405	78.30	32	34	69.29
250	-400	33.17	40	35	87.12

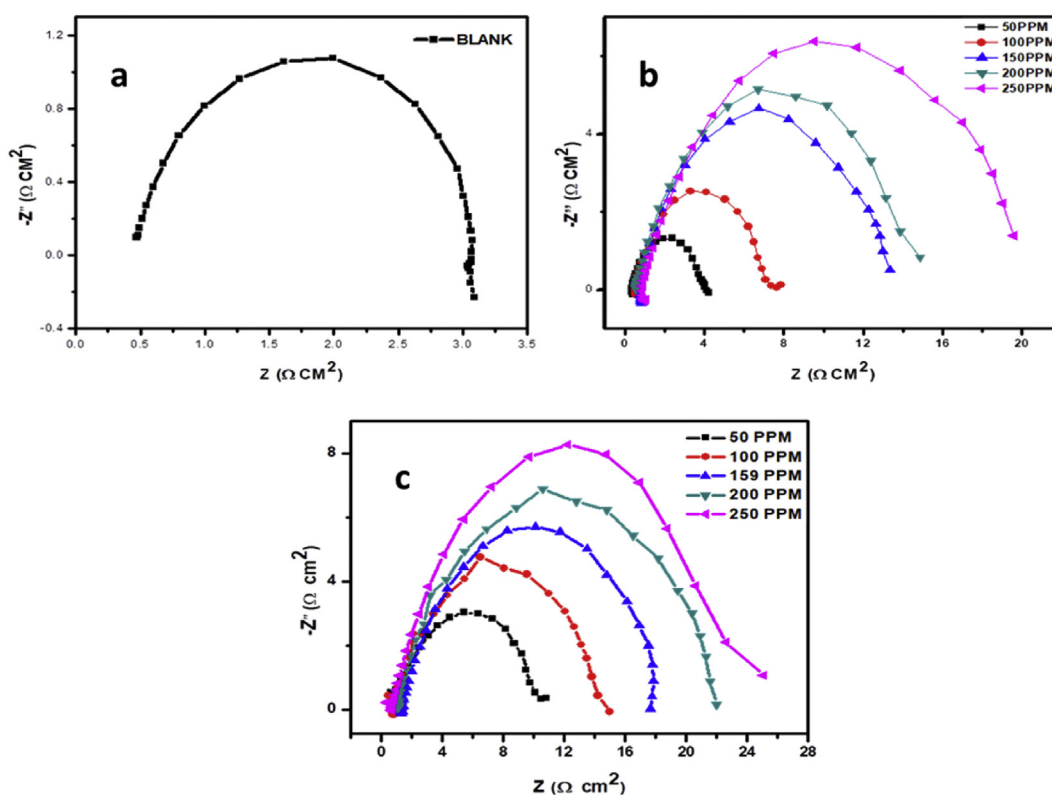


Figure 9. Nyquist plots obtained for mild steel in 1M HCl without a) Blank, and with different concentrations of b) [C₁₆M₁Im] [Br] and c) [C₁₆M₂Im] [Br].

inhibition efficiency, increased with increasing inhibitor concentrations and reached 89.38% for [C₁₆M₂Im] [Br] and 86.15% for [C₁₆M₁Im] [Br]. The order of inhibiting ability is [C₁₆M₂Im] [Br] > [C₁₆M₁Im] [Br] which may be assigned to the structure of the inhibitor [41]. These results suggest a protective layer formed on the metal surface. The obtained results from impedance spectroscopy agree with the polarization and the weight loss studies.

3.4. UV analysis

UV-Visible spectroscopy used to study the interaction between metal and inhibitor molecules. The UV spectrum of the synthesized inhibitors before and after a 1hour immersion of mild steel in 1M HCl solution is shown in Figure 11. All the inhibitors and the inhibited system show a peak at 200–300 nm, which are due to $\pi \rightarrow \pi^*$ transitions [42]. These

transitions exits confirm the formation of the [mild steel-Inhibitor] complex on the mild steel surface [43]. This supports the formation of protective films by [C₁₆M₁Im] [Br] and [C₁₆M₂Im] [Br] due to its active centers on the mild steel surface.

3.5. SEM

Scanning electron microscopy was performed to observe the morphology of the metal surface. The mild steel exposed to 1M HCl solution without and with [C₁₆M₁Im] [Br] and [C₁₆M₂Im] [Br] after 1hour immersion at room temperature is shown in Figure 12. Mild steel in 1M HCl without inhibitor (Figure 12a) is rough and porous, indicating that the mild steel surface has been severely damaged by the acid attack. On the other hand, the damages are reduced and a smooth surface was observed in the presence of [C₁₆M₁Im] [Br] and [C₁₆M₂Im] [Br]

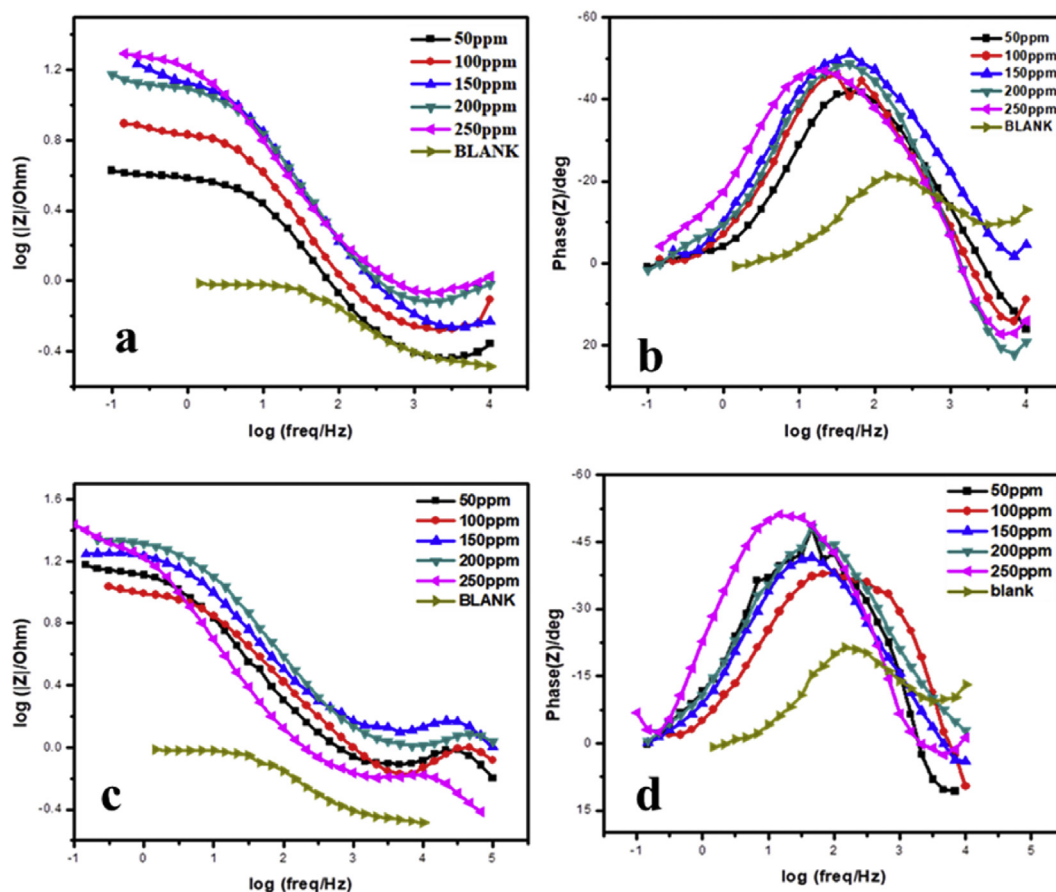


Figure 10. Bode and phase angle diagrams of mild steel in 1M HCl with and without different concentrations of [C₁₆M₁Im] [Br] (a and b) and [C₁₆M₂Im] [Br] (c and d).

Table 6. Impedance parameters for mild steel in 1M HCl in the presence and absence of different concentrations of two inhibitors.

Inhibitor (ppm)	C_{dl} (μFcm^{-2})	R_{ct} (Ωcm^2)	IE (%)
BLANK	0.0381	2.59	-
[C ₁₆ M ₁ Im] [Br]			
50	0.0176	3.75	30.93
100	0.0065	7.33	64.66
150	0.0021	14.28	81.86
200	0.0021	14.27	81.85
250	0.0013	18.71	86.15
[C ₁₆ M ₂ Im] [Br]			
50	0.0019	10.02	74.15
100	0.0013	13.97	81.46
150	0.0011	16.30	84.11
200	0.0008	20.91	87.61
250	0.0006	24.39	89.38

Figure 12b and c demonstrates the formation of a protective layer of adsorbed inhibitor molecules in the mild steel specimen.

3.6. EDAX

EDAX spectra were used to determine the percentage of elements present in the inhibited and uninhibited mild steel surface. The Figure 13a shows EDAX of mild steel in 1M HCl without inhibitor shows O and Cl signals due to the corrosion products (FeO.n H₂O and/or FeCl₂.n H₂O) formed on the metal surface. The Fe wt% is 70.09 which is

less than the inhibited system; this reveals the mild steel surface has been affected in the test solution. On the other hand, the EDAX spectra of Figure 13b and c the best system (mild steel contains 250ppm of [C₁₆M₁Im] [Br] and [C₁₆M₂Im] [Br]) shows the appearance of the N signal of inhibitory molecules. This indicates mild steel surface was covered by inhibitors that can able to protect metal corrosion. Furthermore, peaks of O and Cl do not appear, and high Fe contents also observed which the system inhibits. The above terms confirm the anticorrosive behavior of prepared inhibitors effectively protect mild steel against corrosion.

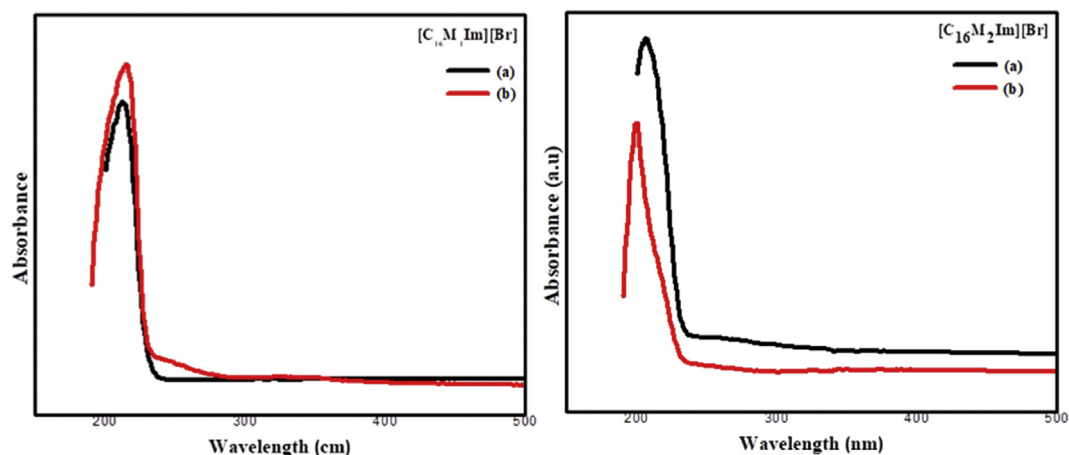


Figure 11. UV spectra of studied inhibitors (a) before, and (b) after immersion of mild steel in 1M HCl.

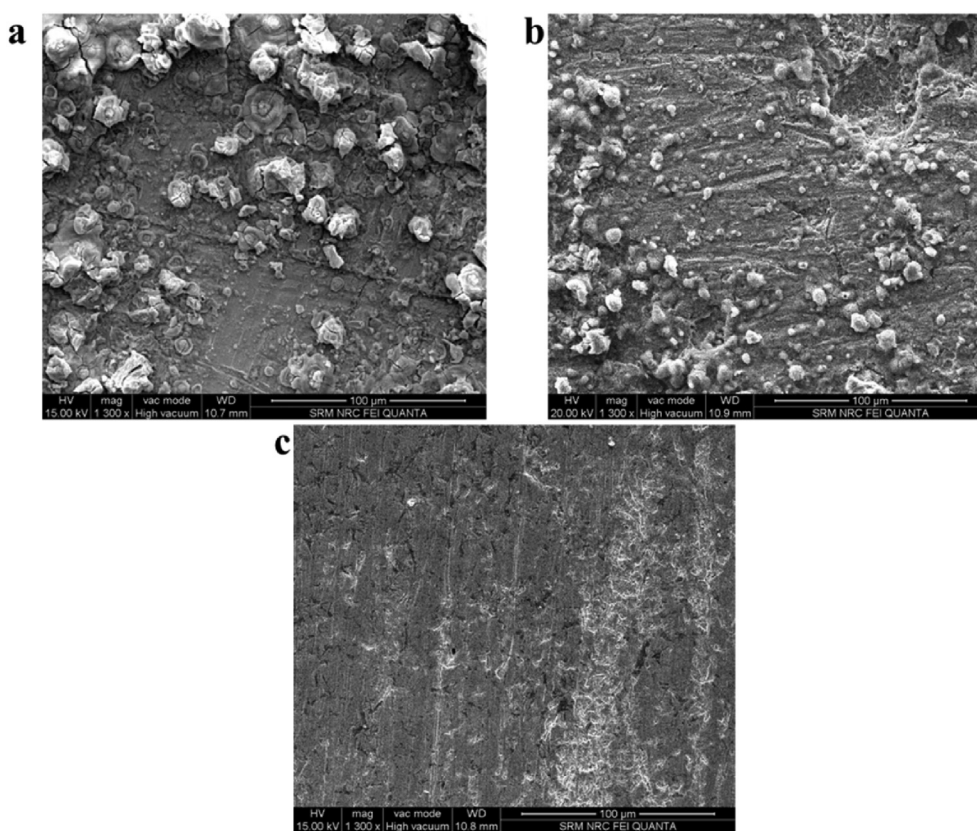


Figure 12. SEM images of mild steel samples: a) after 1h immersion in 1M HCl, b) after 1h immersion in 1M HCl with 250ppm $[C_{16}M_1Im][Br]$ and c) after 1h immersion in 1M HCl with 250ppm $[C_{16}M_2Im][Br]$.

3.7. AFM

AFM images of the mild steel immersed in the absence and presence of $[C_{16}M_1Im][Br]$ and $[C_{16}M_2Im][Br]$ in 1M HCl are shown in Figure 14. The calculated average surface roughness values are listed in Table 7. The mild steel specimen in the test solution without inhibitor (1M HCl) displays an 84.0063 nm surface roughness (Figure 14a). Whereas mild steel immersed in the presence of $[C_{16}M_1Im][Br]$ and $[C_{16}M_2Im][Br]$ (Figure 14b and c), the surface roughness is 59.6871 nm and 50.4605 nm, it was reduced from the blank solution 84.0063 nm. Inhibitive metal surface was improved due to the protective film formed. This tells uninhibited mild steel specimen surface was very rough without inhibitor

due to acid attack. This suggests $[C_{16}M_1Im][Br]$ and $[C_{16}M_2Im][Br]$ inhibitors prevent the metal from acid attack.

3.8. Mechanism of inhibition

Generally, the adsorption process of inhibitors may depend on the size and structure of inhibitor, π electrons in the ring, unshared electrons in the heteroatom, double bond present in the C=N. These factors act as an active center for inhibitor molecules adsorb on mild steel. The adsorption of inhibitors could be considered as either physical or chemical adsorption and mixed type of both physical as well as chemical adsorption take place in the process [44]. First, the physical adsorption is

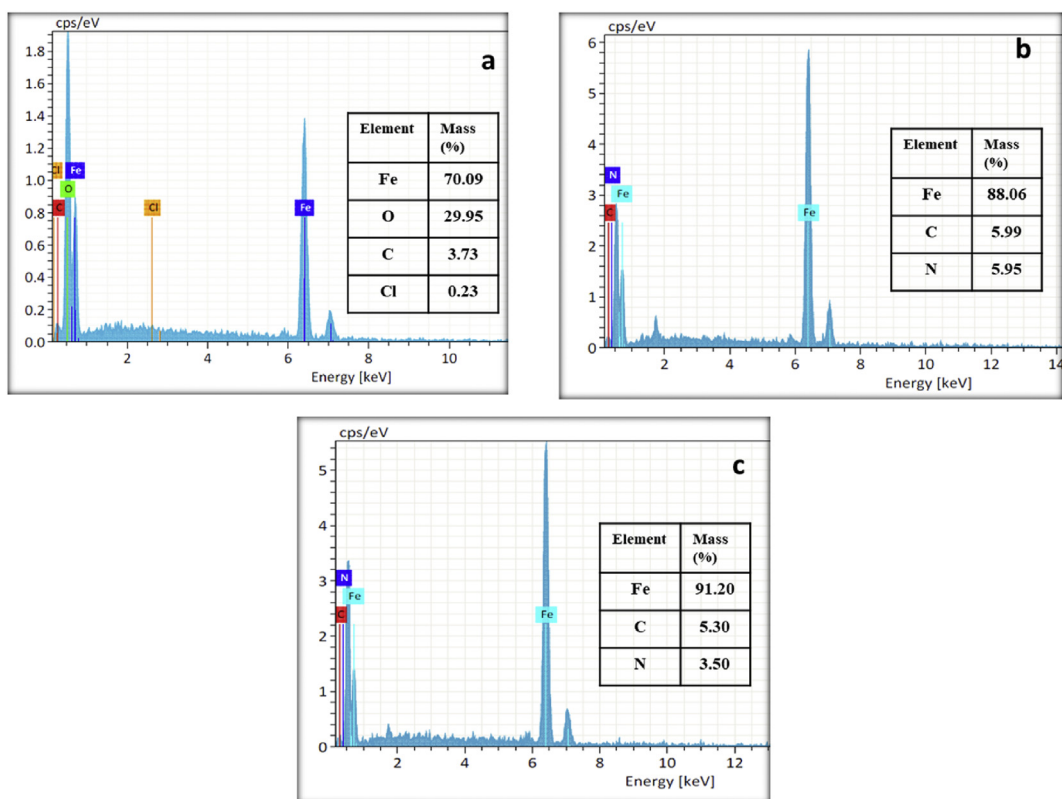


Figure 13. EDAX of mild steel surface: a) after 1h immersion in 1M HCl, b) after 1h immersion in 1M HCl with 250ppm $[C_{16}M_1Im]$ [Br] and c) after 1h immersion in 1M HCl with 250ppm $[C_{16}M_2Im]$ [Br].

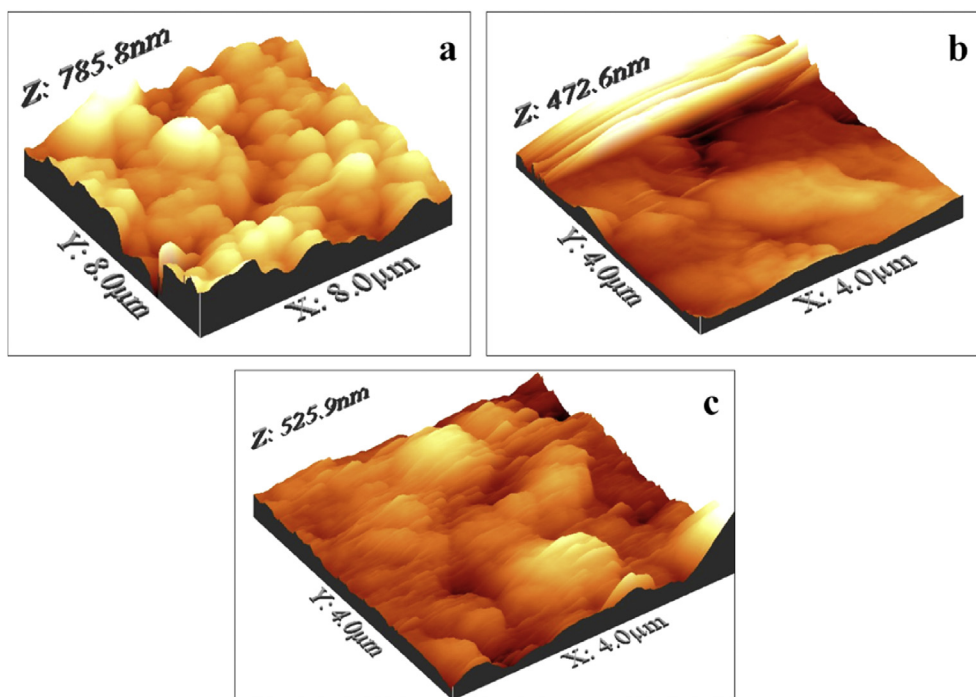


Figure 14. AFM of mild steel in (a) 1M HCl, (b) 1M HCl + $[C_{16}M_1Im]$ [Br] and (c) 1M HCl + $[C_{16}M_2Im]$ [Br].

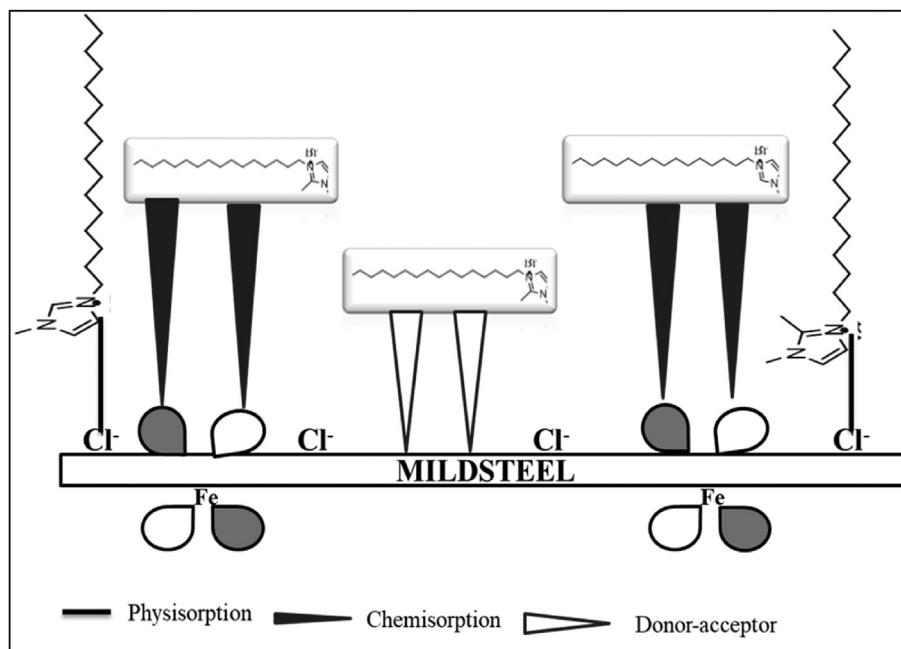
the interaction of two charged species. Later chemical adsorption occurs charge transferring process [45]. According to the literature, inhibitors adsorb on the metal surface on the basis of the following interactions [46],

1. The electrostatic interaction of the charged inhibitor molecules adsorbed with the charged metal surface
2. Interaction of lone pair of electrons in the heteroatom and empty d orbital of the metal surface

Table 7. Average surface roughness values of mild steel in different medium.

Sample	Sa (nm)
1M HCl	84.0063
1M HCl + [C ₁₆ M ₁ Im] [Br]	59.6871
1M HCl + [C ₁₆ M ₂ Im] [Br]	50.4605

following conclusions can be deduced; Inhibition efficiency increases with increasing inhibitor concentrations and decreases with increasing temperature. It reaches maximum inhibition efficiency, 95.35% and 90.67% for [C₁₆M₂Im] [Br] and [C₁₆M₁Im] [Br]. Electrochemical polarization results exhibit that the used inhibitors are mixed type, but predominantly exhibited the anodic inhibitive effect. Impedance studies

**Scheme 2.** Schematic representation of possible adsorption modes of [C₁₆M₁Im] [Br] and [C₁₆M₂Im] [Br] with mild steel surface.

- Donor-acceptor interaction between the π electrons in the benzene ring or double/triple bond in the structure of the inhibitor and empty orbital on the metal surface.

The adsorption of [C₁₆M₁Im] [Br] and [C₁₆M₂Im] [Br] on mild steel surface may be due to their active centers such as a quaternary N⁺ atom, imidazolium ring, and the hydrophobicity (Scheme 2). It is well known that mild steel in 1M HCl solution Cl⁻ ions get adsorb on the metal surface due to the small degree of hydration and make the negative charge on the metal surface. Thus, it is reasonable to assure that the negative charge metal surface enables the adsorption of the positive charges in the inhibitor molecules. Furthermore, the adsorption of inhibitors may take place via interaction between the lone pair of electrons on nitrogen atom present in the [C₁₆M₁Im] [Br] and [C₁₆M₂Im] [Br] and the vacant d orbital of the mild steel surface or donor-acceptor interactions between the π electrons (imidazole ring) and vacant d orbital of the mild steel surface demonstrated in Scheme 2. Since that the inhibitors may be combined with Fe ions to convert Fe-inhibitor complex and adsorbed on the metal surface due to van der Waals force. That could be confirmed by UV spectra [35]. In addition, the prepared [C₁₆M₁Im] [Br] and [C₁₆M₂Im] [Br] inhibitors contain long alkyl chain and methyl substituent may exhibit stronger corrosion inhibition efficiency. This fact can be explained based on the electron density of the inhibitor [46]. It can be concluded, the adsorption of [C₁₆M₁Im] [Br] and [C₁₆M₂Im] [Br] on mild steel was physical adsorption. Ultimately, their adsorption can block the corrosive ions and thus mild steel was effectively protected.

4. Conclusion

The inhibition performance of synthesized compounds, [C₁₆M₁Im] [Br] and [C₁₆M₂Im] [Br] on mild steel in 1M HCl was studied for weight loss, electrochemical measurements, UV and surface studies. The

indicate charge transfer resistance increased with increasing inhibitor concentrations, suggests inhibitor adsorbed on the surface of the metal. The inhibitors adsorbed on the mild steel surface obey the Langmuir isotherm. The formation of the [MS-Inhibitor] complex in the mild steel specimen was confirmed by UV spectra. An SEM-EDAX and AFM result confirms a protective layer formed on the mild steel surface. Inhibition efficiency follows the order of [C₁₆M₁Im] [Br] < [C₁₆M₂Im] [Br], which is correlated with methyl substituents increase the electron density of the inhibitor compound.

Declarations

Author contribution statement

N. Subasree: Conceived and designed the experiments; Performed the experiments; Wrote the paper.

J. Arockia Selvi: Conceived and designed the experiments; Analyzed and interpreted the data.

Funding statement

This research did not receive any specific grant from funding agencies in the public, commercial, or not-for-profit sectors.

Competing interest statement

The authors declare no conflict of interest.

Additional information

No additional information is available for this paper.

Acknowledgements

We acknowledge the Nanotechnology Research Centre (NRC), SRMIST for providing AFM and SEM-EDAX facilities. The authors would like to thank Dr. Gopal Chandru Senadi, Department of chemistry, SRMIST for his help in the analysis of NMR spectra and Dr. M. Mariappan, Department of chemistry, SRMIST for UV analysis.

References

- T. Peme, L. Olasunkanmi, I. Bahadur, A. Adekunle, M. Kabanda, E. Ebenso, Adsorption and corrosion inhibition studies of some selected dyes as corrosion inhibitors for mild steel in acidic medium: gravimetric, electrochemical, quantum chemical studies and synergistic effect with iodide ions, *Molecules* 20 (2015) 16004–16029.
- S.M. Tawfik, Alginate surfactant derivatives as an ecofriendly corrosion inhibitor for carbon steel in acidic environments, *RSC Adv.* 5 (2015) 104535–104550.
- Mohammed H. Othman Ahmed, Ahmed A. Al-Amiery, Yasmin K. Al-Majedy, Abdul Amir H. Kadhum, Abu Bakar Mohamad, Tayser Sumer Gaaz, Synthesis and characterization of a novel organic corrosion inhibitor for mild steel in 1 M hydrochloric acid, *Results Phys.* 8 (2018) 728–733.
- Yasser Karzazi, Mohammed El Alaoui Belghiti, Ali Dafali, Belkheir Hammouti, A theoretical investigation on the corrosion inhibition of mild steel by piperidine derivatives in hydrochloric acid solution, *J. Chem. Pharmaceut. Res.* 6 (2014) 689–696.
- Madhusudan Goyal, Sudershan Kumar, Indra Bahadur, Chandrabhan Verma, Eno E. Ebenso, Organic corrosion inhibitors for industrial cleaning of ferrous and non-ferrous metals in acidic solutions: a review, *J. Mol. Liq.* 256 (2018) 565–573.
- F. Mohsenifar, H. Jafari, K. Sayin, Investigation of thermodynamic parameters for steel corrosion in acidic solution in the presence of N, N'-Bis (phloracetophenone)-1, 2 propanediamine, *J. Bio Tribo-Corrosion* 2 (2016) 1.
- R. Ganapathi Sundaram, M. Sundaravadivelu, Anticorrosion activity of 8-quinoline sulphonyl chloride on mild steel in 1 M HCl solution, *J. Metall.* (2016).
- B.M. Mistry, N.S. Patel, S. Sahoo, S. Jauhari, Experimental and quantum chemical studies on corrosion inhibition performance of quinoline derivatives for MS in 1N HCl, *Bull. Mater. Sci.* 35 (2012) 459–469.
- C.A. Loto, R.T. Loto, Corrosion inhibition of thiourea and thiazazole derivatives: a review, *J. Mater. Environ. Sci.* 3 (2012) 885–894.
- N. Wazzan, S. Al-Mhyawi, Application of newly quiniline-3-carbonitriles as corrosion inhibitors on mild steel in 1.0 M HCl: electrochemical measurements, HF and DFT/B3LYP calculations, *Int. J. Electrochem. Sci.* 12 (2017) 9812–9828.
- R. Ratti, Ionic liquids: synthesis and applications in catalysis, *Adv. Chem.* (2014).
- M. Koel, Ionic liquids in chemical analysis, *Crit. Rev. Anal. Chem.* 35 (2005) 177–192.
- C. Verma, I.B. Obot, Indra Bahadur, El-Sayed M. Sherif, E.E. Ebenso, Choline based ionic liquids as sustainable corrosion inhibitors on mild steel surface in acidic medium: gravimetric, electrochemical, surface morphology, DFT and Monte Carlo simulation studies, *Appl. Surf. Sci.* 457 (2018) 134–149.
- C. Verma, E.E. Ebenso, M.A. Quraishi, Ionic liquids as green corrosion inhibitors for industrial metals and alloys. *Green Chemistry, IntechOpen*, 2018.
- N.V. Likhanova, O. Olivares-Xometl, D. Guzmán-Lucero, M.A. Domínguez-Aguilar, N. Nava, M. Corrales-Luna, M.C. Mendoz, Corrosion inhibition of carbon steel in acidic environment by imidazolium ionic liquids containing vinyl-hexafluorophosphate as anion, *Int. J. Electrochem. Sci.* 6 (2011) 4514–4536.
- C. Verma, E.E. Ebenso, M.A. Quraishi, Ionic liquids as green and sustainable corrosion inhibitors for metals and alloys: an overview, *J. Mol. Liq.* 233 (2017) 403–414.
- A. Atta, G. El-Mahdy, H. Al-Lohedan, A. Ezzat, A new green ionic liquid-based corrosion inhibitor for steel in acidic environments, *Molecules* 20 (2015) 11131–11153.
- A.S. Fouda, M.A. Migahed, A.A. Atia, I.M. Mousa, Corrosion inhibition and adsorption behavior of some cationic surfactants on carbon steel in hydrochloric acid solution, *J. Bio Tribo-Corrosion* 2 (2016) 22.
- N. Kovačević, A. Kokalj, Chemistry of the interaction between azole type corrosion inhibitor molecules and metal surfaces, *Mater. Chem. Phys.* 137 (2012) 331–339.
- F.A. Azeez, O.A. Al-Rashed, A.A. Nazeer, Controlling of mild-steel corrosion in acidic solution using environmentally friendly ionic liquid inhibitors: effect of alkyl chain, *J. Mol. Liq.* 265 (2018) 654–663.
- P. Arellanes-Lozada, O. Olivares-Xometl, N.V. Likhanova, I.V. Lijanova, J.R. Vargas-García, R.E. Hernández-Ramírez, Adsorption and performance of ammonium-based ionic liquids as corrosion inhibitors of steel, *J. Mol. Liq.* 265 (2018) 151–163.
- O. Olivares-Xometl, E. Álvarez-Álvarez, N.V. Likhanova, I.V. Lijanova, R.E. Hernández-Ramírez, P. Arellanes-Lozada, J.L. Varela-Caselis, Synthesis and corrosion inhibition mechanism of ammonium-based ionic liquids on API 5L X60 steel in sulfuric acid solution, *J. Adhes. Sci. Technol.* 32 (2018) 1092–1113.
- Jitendra Kumar Singh, Rahul Kumar Sharma, Pushpal Ghosh, Ashwani Kumar, Mohammed Latif Khan, Imidazolium based ionic liquids: a promising green solvent for water hyacinth biomass deconstruction, *Front. Chem.* 6 (2018) 548.
- Carolina Zuriaga-Monroy, Raúl Oviedo-Roa, Luisa E. Montiel-Sánchez, Araceli Vega-Paz, Jesus Marin-Cruz, Jose-Manuel Martinez-Magadan, Theoretical study of the aliphatic-chain length's electronic effect on the corrosion inhibition activity of methylimidazole-based ionic liquids, *Ind. Eng. Chem. Res.* 55 (2016) 3506–3516.
- Hojat Jafari, Farhhad Mohsenifar, Koray Sayin, Effect of alkyl chain length on adsorption behavior and corrosion inhibition of imidazoline inhibitors, *Iran. J. Chem. Chem. Eng. (Int. Engl. Ed.)* 37 (2018) 85–103.
- C. Subramanian, Localized pitting corrosion of API 5L grade A pipe used in industrial fire water piping applications, *Eng. Fail. Anal.* 92 (2018) 405–417.
- R. Marsha Cole, Min Li, Bilal El-Zahab, Marlene E. Janes, Daniel Hayes, Isiah M. Warner, Design, synthesis, and biological evaluation of β -lactam antibiotic-based imidazolium-and pyridinium-type ionic liquids, *Chem. Biol. Drug Des.* 78 (2011) 33–41.
- A. Zarrouk, H. Zarrok, R. Salghi, N. Bouroumane, B. Hammouti, S.S. Al-Deyab, R. Touzani, The Adsorption and Corrosion Inhibition of 2-[bis-(3, 5-dimethyl-pyrazol-1-ylmethyl)-amino]-pentanedioic acid on carbon steel corrosion in 1.0 m HCl, *Int. J. Electrochem. Sci.* 7 (2012) 10215–10232.
- A.S. Fouda, M.T. Mohamed, M.R. Soltan, Role of some benzohydrazide derivatives as corrosion inhibitors for carbon steel in HCl solution, *J. Electrochem. Sci. Technol.* 4 (2013) 61–70.
- I. Ichchou, L. Larabi, H. Rouabhi, Y. Harek, A. Fellah, Electrochemical evaluation and DFT calculations of aromatic sulfonohydrazides as corrosion inhibitors for XC38 carbon steel in acidic media, *J. Mol. Struct.* 1198 (2019) 126898.
- Nurul Izni Kairi, Kassim Jain, The effect of temperature on the corrosion inhibition of mild steel in 1 M HCl solution by curcuma longa extract, *Int. J. Electrochem. Sci.* 8 (2013) 7138–7155.
- E.E. Oguzie, Inhibition of acid corrosion of mild steel by Telfaria occidentalis extract, *Pigment Resin Technol.* 34 (2005) 321–326.
- A. Zarrouk, M. Messali, H. Zarrok, R. Salghi, A.A. Ali, B. Hammouti, S.S. Al-Deyab, F. Bentiss, Synthesis, characterization and comparative study of new functionalized imidazolium-based ionic liquids derivatives towards corrosion of C38 steel in molar hydrochloric acid, *Int. J. Electrochem. Sci.* 7 (2012) 6998–7015.
- Sárka Langová, Petr Pánek, Fojtásková Jana, Sárka Vicherková, Alkylimidazolium bromides as corrosion inhibitors for mild steel in acidic medium, *Trans. Indian Inst. Met.* 71 (2018) 1371–1378.
- Yangyang Guo, Bin Xu, Ying Liu, Wenzhong Yang, Xiaoshuang Yin, Yun Chen, Jinxun Le, Zhihao Chen, Corrosion inhibition properties of two imidazolium ionic liquids with hydrophilic tetrafluoroborate and hydrophobic hexafluorophosphate anions in acid medium, *J. Ind. Eng. Chem.* 56 (2017) 234–247.
- S. Yesudass, L.O. Olasunkanmi, I. Bahadur, M.M. Kabanda, I.B. Obot, E.E. Ebenso, Experimental and theoretical studies on some selected ionic liquids with different cations/anions as corrosion inhibitors for mild steel in acidic medium, *J. Taiwan Inst. Chem. Eng.* 64 (2016) 252–268.
- Jagadeesan Saranya, Murugaiyan Sowmiya, Palanisamy Sounthari, Kandhasamy Parameswari, Subramanian Chitra, Kittusamy Senthilkumar, N-heterocycles as corrosion inhibitors for mild steel in acid medium, *J. Mol. Liq.* 216 (2016) 42–52.
- Hussein Jwad Habeeb, Hasan Mohammed Luaibi, Thamer Adnan Abdullah, Rifaat Mohammad Dakhil, Abdul Amir H. Kadhum, Ahmed A. Al-Amiery, Case study on thermal impact of novel corrosion inhibitor on mild steel, *Case Stud. Thermal Eng.* 12 (2018) 64–68.
- Wewei Zhang, Hui-Jing Li, Meirong Wang, Li-Juan Wang, Ai-Han Zhang, Yan-Chao Wu, Highly effective inhibition of mild steel corrosion in HCl solution by using pyrido [1, 2-a] benzimidazoles, *New J. Chem.* 43 (2019) 413–426.
- Fan Zhang, Yongming Tang, Ziyi Cao, Wenheng Jing, Zhenglei Wu, Yizhong Chen, Performance and theoretical study on corrosion inhibition of 2-(4-pyridyl)-benzimidazole for mild steel in hydrochloric acid, *Corrosion Sci.* 61 (2012) 1–9.
- Takahiro Ishizaki, Junko Hieda, Nagahiro Saito, Naobumi Saito, Osamu Takai, Corrosion resistance and chemical stability of super-hydrophobic film deposited on magnesium alloy AZ31 by microwave plasma-enhanced chemical vapor deposition, *Electrochim. Acta* 55 (2010) 7094–7101.
- Yue Meng, Wenbo Ning, Bin Xu, Wenzhong Yang, Kegui Zhang, Yun Chen, Lihua Li, Xi Liu, Jinhong Zheng, Yimin Zhang, Inhibition of mild steel corrosion in hydrochloric acid using two novel pyridine Schiff base derivatives: a comparative study of experimental and theoretical results, *RSC Adv.* 68 (2017) 43014–43029.
- Jiyaul Haque, V. Srivastava, Chandrabhan Verma, H. Lgaz, R. Salghi, M.A. Quraishi, N-Methyl-N, N, N-trioctylammonium chloride as a novel and green corrosion inhibitor for mild steel in an acid chloride medium: electrochemical, DFT and MD studies, *New J. Chem.* 22 (2017) 13647–13662.
- Hülya Keleş, Duygu Melis Emir, Mustafa Keleş, A comparative study of the corrosion inhibition of low carbon steel in HCl solution by an imine compound and its cobalt complex, *Corrosion Sci.* 101 (2015) 19–31.
- Lei Zhang, He Yi, Yanqiu Zhou, Ranran Yang, Qiangbin Yang, Dayong Qing, Qianhe Niu, A novel imidazoline derivative as corrosion inhibitor for P110 carbon steel in hydrochloric acid environment, *Petroleum* 3 (2015) 237–243.
- Amrishi Singh, K.R. Ansari, Xihua Xu, Zhipeng Sun, Ashok Kumar, Yuanhua Lin, An impending inhibitor useful for the oil and gas production industry: weight loss, electrochemical, surface and quantum chemical calculation, *Sci. Rep.* 1 (2017) 14904.